Two color multichannel heterodyne interferometer set up for high spatial resolution electron density profile measurements in TJ-II[a)]

P. Pedreira,[1,b)] L. Esteban,[2] A. R. Criado,[1] P. Acedo,[1] M. Sánchez,[2] and J. Sánchez[2]
[1]*Department of Electronics Technology, Universidad Carlos III de Madrid, Leganes, Madrid 28911, Spain*
[2]*Laboratorio Nacional de Fusión por ConfinamientoMagnético-CIEMAT, Madrid 28040, Spain*

(Presented 17 May 2010; received 17 May 2010; accepted 14 June 2010; published online 5 October 2010)

A high spatial resolution two color [CO_2, $\lambda=10.6$ μm/Nd:YAG (Nd:YAG denotes neodymium-doped yttrium aluminum garnet), and $\lambda=1.064$ μm] expanded-beam multichannel heterodyne interferometer has been installed on the TJ-II stellarator. Careful design of the optical system has allowed complete control on the evolution of both Gaussian beams along the interferometer, as well as the evaluation and optimization of the spatial resolution to be expected in the measurements. Five CO_2 (measurement) channels and three Nd:YAG (vibration compensation) channels have been used to illuminate the plasma with a probe beam of 100 mm size. An optimum interpolation method has been applied to recover both interferometric phasefronts prior to mechanical vibration subtraction. The first results of the installed diagnostic are presented in this paper. © *2010 American Institute of Physics.* [doi:10.1063/1.3475729]

I. INTRODUCTION

Multichannel heterodyne laser interferometers are widely used to provide information on the electron density profiles in fusion plasmas both in stellarators[1] and tokamaks.[2] In the past years we have witnessed an increasing interest in the development of interferometric density profile measurement systems with high spatial resolution for short scale-length ($\sim$1–5 mm) density fluctuation studies.[3] In all these systems, the mechanical vibration compensation appears as one of the main issues in order to obtain the required high spatial resolution, as the residual mechanical noise (uncompensated vibration) degrades the measurements.[1,3] On the other hand, a systematic approach to the evaluation of the ultimate spatial resolution of these systems is needed in order to design diagnostics for the desired performances.[4]

In this work, we describe the design, installation and first results of an expanded-beam CO_2/Nd:YAG (YAG denotes yttrium aluminum garnet) heterodyne interferometer for the TJ-II stellarator ($R=1.5$ m, $a<0.2$, $B=1$ T) to perform high spatial resolution electronic density profile measurements. The interferometer has been designed in order to control the Gaussian characteristics of both wavelengths along the setup to obtain the desired spatial resolution. Optical design software, ZEMAX, is used for the optimization of the interferometer: Gaussian beam propagation through the port, the magnification and demagnification telescopic systems, and the study of aberrations.[5]

The design of the diagnostic for the desired spatial resolution performance has involved an adequate choice of the demagnification system and the design of custom-made detector arrays (dimensions and separation between adjacent elements). The *a priori* determination of the spatial resolution of the design is based on the theory of Gaussian beams and the diffraction-limited criterion,[6] taking also into account the detectors characteristics. This systematic design, along with preliminary calibration studies[4] has led to an optical system with the desired performances.

A final step in the diagnostic design has involved the study of different reconstruction interpolation methods to retrieve the interferometric heterodyne phase profiles for each wavelength. Polinomic and spline interpolation methods have been evaluated, but the best results are obtained through the application of the Shannon–Whittaker sampling theorem,[7] that has already been applied in other multichannel interferometric schemes for studies on retrieving spatial phasefronts.[8] Optimum phasefronts reconstructions are the key to proper mechanical vibration cancellation along the complete wavefront as well as to obtain the line density integral profile with a high accuracy.

II. MULTICHANNEL HETERODYNE LASER INTERFEROMETRIC DIAGNOSTIC

A. Interferometer optical setup

Figure 1 shows the optical layout of the expanded beam multichannel heterodyne laser interferometer. The laser sources are the following. For the measurement wavelength, a CO_2 laser, Model Merit from Access Laser Company ($\lambda=10.6$ μm, 9 W, beam diameter=2.4 mm, beam divergence-full angle=5.5 mrad) and, for the mechanical vibration compensation wavelength, a Nd:YAG laser, model IRCL-300-1064-S from Crystal Laser (1.064 μm, 300 mW, beam diameter=0.45 mm, beam divergence-full angle=3.6 mrad). A third laser source (He–Ne: 0.633 μm) is used to

[a)]Contributed paper, published as part of the Proceedings of the 18th Topical Conference on High-Temperature Plasma Diagnostics, Wildwood, New Jersey, May 2010.
[b)]Electronic mail: ppedreir@ing.uc3m.es.

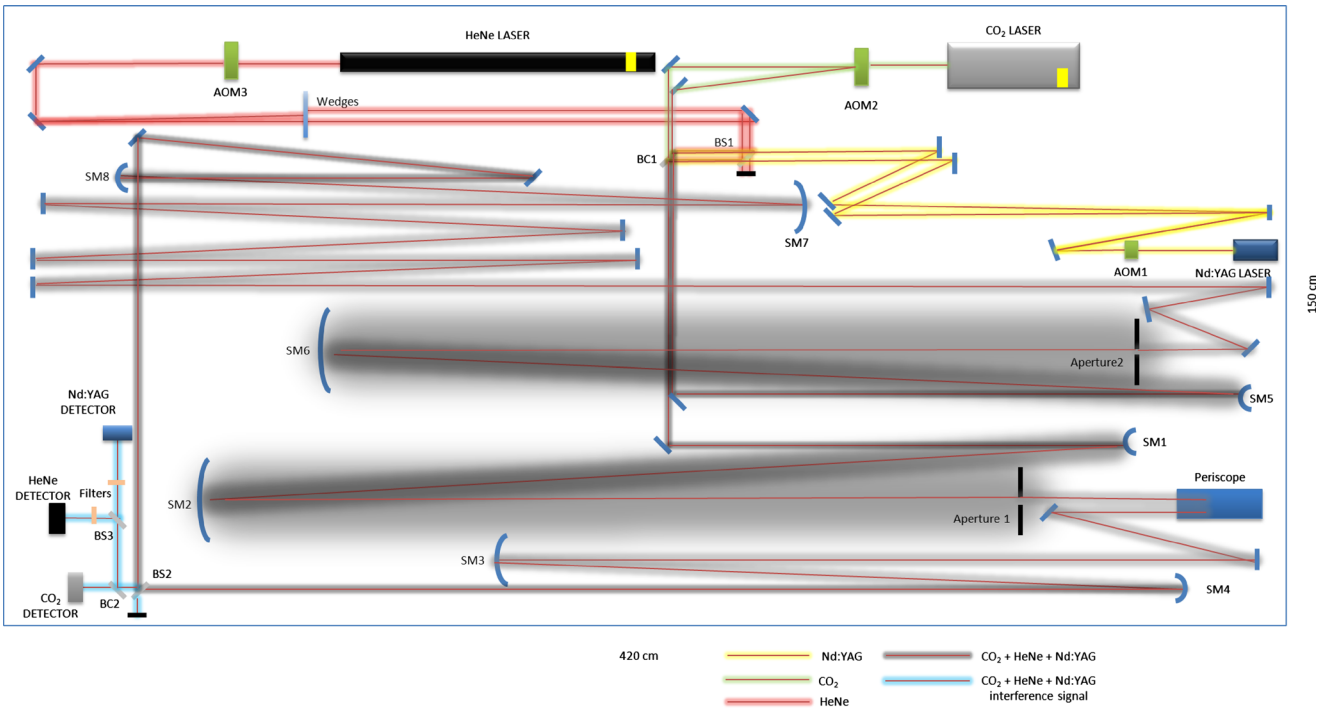

FIG. 1. (Color online) Optical Layout of the multichannel heterodyne laser interferometer.

aid in the alignment of the system and also to separately study phenomena relevant to the interferometric diagnostics which is also an objective of this system, i.e., the influence of the speckle in the spatial resolution, diffraction due to apertures, and the refraction index variation associated to the ZnSe plasma access window heating.

CO_2 and Nd:YAG wavelengths pass through the acousto-optic modulators separating the input beams into a zeroth and first diffraction order beams with a 40 MHz separation frequency for CO_2 and 39.9 MHz for Nd:YAG. In both reference and measurement arms, the beams are magnified $\times 7$ by a telescopic system that consists of a pair of convex and concave spherical mirrors. This fact causes decreases in the divergence for both wavelengths so that the probe beams increase insignificantly in size when propagating through the rest of the system. Next, the beams pass through a rectangular aperture of 10×100 mm^2 in order to shape the spot that illuminates the plasma. For this first campaign, the plasma access window (300 mm large) is shared with the already operational single channel system,[9] and the spot size that passes through the plasma has been kept to 100 mm. This elliptical probe beam is steered to the plasma access window by a periscope. This beam is reflected back by a large rectangular mirror located on the top of the port toward the periscope again. Then, the probe beam is demagnified $\times 3.5$ by another pair of concave spherical mirrors. The reference arm is shaped and demagnified in the same way as the measurement arm. After this, both arms are steered to a beam splitter for recombination. The final sizes of the spots match the detector arrays dimensions (4×35 mm^2). Table I shows the vertical sizes of the CO_2 and Nd:YAG beams for different points along the arms of the interferometer.

The beam sizes of each wavelength are measured with their corresponding array and with the help of a chopper. Each array is placed on a manual linear translation stage. This setup allows the wavefront to be sampled using the 32 detector elements of the arrays, to fit the acquired samples a Gaussian profile and hence, to determine the radius of the $1/e^2$ contour, w(z). The difference between experimental measurements and simulated values is around 1%. Furthermore, it is important to note that the actual dimensions of the beams along the diagnostics perfectly match the preliminary optical simulations validating the methodology for the diagnostics optical design.

B. Signal detection and multichannel phase detection system

Two linear arrays are used to measure both interferometric signals. The Nd:YAG signal is detected using a PIN array of 35 elements (4.4×0.9 mm^2 each one). The CO_2 detector array, a custom device designed with the collaboration of Vigo Systems is made up of 32 photovoltaic elements (3.3

TABLE I. Vertical sizes of CO_2 and Nd:YAG beams in the principal localizations of the interferometric system.

Position	Wavelength	Vertical size (mm)
Magnification system	CO_2	147.68
	Nd:YAG	138.46
Periscope	CO_2	98.40
	Nd:YAG	100.42
Plasma	CO_2	104.62
	Nd:YAG	104.72
Beam splitter (measurment arm)	CO_2	35.47
	Nd:YAG	34.12
Beam splitter (reference arm)	CO_2	36.42
	Nd:YAG	34.53

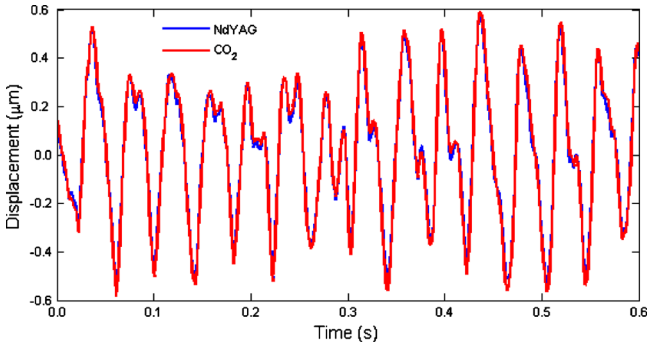

FIG. 2. (Color online) Measurement of the mechanical vibrations of the CO_2 and Nd:YAG laser interferometer.

$\times 0.5$ mm^2) with high responsivity that does not require biasing nor cooling for a compact multichannel detection system. Such an array is mounted on a butterfly package to obtain high bandwidth and low crosstalk between channels. The spacing between elements is 1 mm in both arrays. The output signals of the arrays are amplified and filtered by custom-made signal conditioning stages to obtain the signal levels required at the multichannel phase detector inputs. This signal conditioning involves several low noise amplifiers (for a total gain of 70 dB) and a bandpass filter with 20 MHz bandwidth. The multichannel phase detection system[4,10] is based on a field programmable gate array (FPGA).

III. EXPERIMENTAL RESULTS

The interferometric diagnostic described has already been installed in the TJ-II stellarator and it is scheduled to be operational during the last weeks of the 2010 Spring Campaign. The first tests on the complete system have involved validation of the spatial resolution for the current diagnostic studying the far field divergence of a truncated Gaussian beam. The estimated results for such interferometric system for TJ-II are 32 channels with a 4–5 mm chord lateral separation and line integral error measurements $<10^{17}$ m^{-2}. These results demonstrate both that the spatial resolution requirements for the diagnostics installed in the TJ-II are met and that the design methodology used is valid and could be used for the design of other high spatial resolution systems.

In a multichannel interferometric system, a correct mechanical vibration cancellation leads to a precise good determination of spatial resolution. As a consequence of this, the application of the ideal reconstruction algorithm will provide high accuracy when obtaining the line integral density profile. Validation of proper mechanical vibration subtraction for the installed system is done channel by channel along the complete phasefront of the interferometric system. In Fig. 2, we show an example of the static performance of the system. In this figure we can see the output for both wavelengths (CO_2: red line, Nd:YAG: blue line), and how both are able to track the vibrations of the system. In Fig. 3, we show the

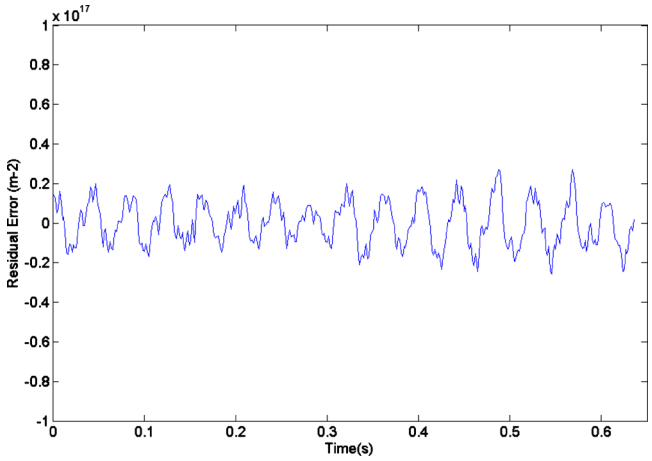

FIG. 3. (Color online) Residual error in the line-integrated electron density measurement due to the uncompensated vibrations.

residual error in the line-integrated electron density measurement associated to the uncompensated vibrations. These results anticipate an RMS error in the line integral measurement within the 1×10^{16} m^{-2} range, due to the uncompensated vibrations. Figure 3 shows the residual error in the cancellation process of the in line-integrated electron density units.

With the results shown above, we can conclude that the high spatial resolution multichannel system is ready for operation. The first electron density measurements are expected during the coming weeks once the interferometer phase detection system is finally integrated in the TJ-II stellarator diagnostic system.

ACKNOWLEDGMENTS

This work was supported by Spanish Ministry of Education and Science (Grant No. ENE2006-13559FTN). The authors would also like to acknowledge the help of Ernesto Garcia Ares and Jose Ramon Lopez Fernandez for setting up the signal conditioning systems.

[1] K. Tanaka, A. L. Sanin, L. N. Vyacheslavov, Y. Akiyama, K. Kawahata, T. Tokuzawa, Y. Ito, and S., Okajima, Rev. Sci. Instrum. **75**, 3429 (2004).
[2] J. H. Irby, E. S. Marmar, E. Sevillano, and S. M. Wolfe, Rev. Sci. Instrum. **59**, 1568 (1988).
[3] J. H. Irby, R. Murray, P. Acedo, and H. Lamela, Rev. Sci. Instrum. **70**, 699 (1999).
[4] P. Acedo, P. Pedreira, A. R. Criado, H. Lamela, M. Sánchez, and J. Sánchez, Rev. Sci. Instrum. **79**, 10E713 (2008).
[5] P. Pedreira, L. Esteban, A. R. Criado, P. Acedo, M. Sánchez, and J. Sánchez, Proceedings of the 36th EPS Conference on Plasma Physics, Sofia, 29 June–3 July 2009, ECA, Vol. 33E, p. 4.187.
[6] E. M. Drège, N. G. Skinner, and D. M. Byrne, Appl. Opt. **39**, 4918 (2000).
[7] J. W. Goodman, *Introduction to Fourier Optics* (McGraw-Hill, New York, 1968).
[8] P. E. Young, D. P. Neikirk, P. P. Tong, D. B. Rutledge, and N. C. Luhnmann, Rev. Sci. Instrum. **56**, 81 (1985).
[9] P. Acedo, H. Lamela, M. Sánchez, T. Estrada, and J. Sánchez, Rev. Sci. Instrum. **75**, 4671 (2004).
[10] L. Esteban, M. Sánchez, J. A. López, O. Nieto-Taladriz, and J. Sánchez, Fusion Eng. Des. **85**, 328 (2010).